Hydrol. Earth Syst. Sci. Discuss., 9, 11551–11581, 2012
www.hydrol-earth-syst-sci-discuss.net/9/11551/2012/
doi:10.5194/hessd-9-11551-2012

Hydrology and Earth System Sciences Discussions

Maximum entropy production: can it be used to constrain conceptual hydrological models?

M. C. Westhoff and E. Zehe

Department of Hydrology, Institute for Water and River Basin Management, Karlsruhe Institute of Technology – KIT, Kaiserstr. 12, 76131 Karlsruhe, Germany

Received: 20 September 2012 – Accepted: 24 September 2012 – Published: 9 October 2012

Correspondence to: M. C. Westhoff (martijn.westhoff@kit.edu)

Published by Copernicus Publications on behalf of the European Geosciences Union.

Abstract

In recent years, optimality principles have been proposed to constrain hydrological models. The principle of Maximum Entropy Production (MEP) is one of the proposed principles and is subject of this study. It states that a steady state system is organized in such a way that entropy production is maximized. However, within hydrology, tests against observations are still missing. The aim of this paper is to test the MEP principle to reduce equifinality of a simple conceptual (bucket) model. We used the principle of maximizing power, which is equivalent to MEP when a constant temperature is assumed. Power is determined by multiplying a flux with its gradient. We thus defined for each flux in the model a gradient and checked if parameter sets that maximize power also reproduce the observed water balance. Subsequently we concluded that with the used model concept, this does not work. It would be easy to reject the MEP hypothesis to explain our findings, but we believe that our test is incomplete.

By referring to the flaws in our own model concept, we believe that many issues can be learned about how to use MEP to constrain hydrological models. Among others, the most important are: (1) fluxes should be defined as a gradient divided by a resistance, where the flux feeds back on the gradient; (2) there should be a trade-off between two or more different fluxes, where, in principle, only one resistance can be optimized and (3) each process should have the right degrees of freedom: what are the feedbacks on this flux and what limits the flux?

1 Introduction

Traditionally, hydrology is concerned with predicting extremes or water balances for water resources management. But the simplified model structures induce errors, while model parameters are often calibrated on an observed integrated catchment response (often discharge). In recent years, optimality based principles have been suggested to be able to better estimate model parameters and thus model behaviour (e.g. McDonnell

HESSD
9, 11551–11581, 2012

et al., 2007; Kleidon and Schymanski, 2008; Clark et al., 2011; Schaefli et al., 2011; Thompson et al., 2011).

The basic idea of optimality principles is that nature organizes itself in such a way that its functioning is optimal under given external forcing during steady state conditions. This can be simulated, by taking into account competition between different plant species or trade-offs between fluxes that are driven by different gradients. This competition should then be translated into an objective function. For example, Rodriguez-Iturbe et al. (1999), Porporato et al. (2001) and Caylor et al. (2009) minimized water stress as the objective function for vegetation in (semi-)arid areas. Maximum transpiration and minimal water and oxygen stress has been used by Brolsma and Bierkens (2007), who simulated the competition between two vegetation species, while Schymanski et al. (2009b) optimized net carbon profit under given environmental conditions. Another proposed organizing principle is the Maximum Entropy Production principle (MEP) (McDonnell et al., 2007; Kleidon and Schymanski, 2008; Kleidon, 2009, 2010a,b; Zehe and Sivapalan, 2009; Schaefli et al., 2011). However, in the hydrological community it remained – so far – mainly on the visionary level.

The above mentioned studies are just a few examples of optimality based models (mainly) in ecohydrology. For a more extensive review, the reader is referred to e.g. Schymanski et al. (2009a).

Several different optimality principles have been used so far, and the question is which one to use. Paik and Kumar (2010) stated that many optimality principles are useful, but that MEP has at least a physical background. Although the physical background of MEP is still under debate, (e.g. Dewar, 2009, suggests that MEP is rather a statistical principle, where the state of MEP is just the most probable one), it seems a useful principle, and many of the proposed objective functions are related to MEP (Dewar, 2010). It is also the objective function used in this study.

The principle of MEP relies on the fact that a gradient drives a flux, while the same flux depletes the gradient. This has been clearly shown by Paltridge (1979) and Lorenz et al. (2001) who used the principle to explain the observed atmospheric movement

HESSD
9, 11551–11581, 2012

from the equator to the poles for planetary systems. Dewar (2010) showed how MEP could be used for plant optimization at different scales, but a comparison with observations was missing. A more hydrological application was formulated by Kleidon and Schymanski (2008), who used the principle to describe the partitioning between runoff and evaporation, but they also did not test their theory with observations. Schymanski et al. (2010) used a simple 2-box model and MEP to predict pattern formation of vegetation in semiarid regions, which gave similar results as the large scale distributed model of Klausmeier (1999).

Comparison with observation has been done by Zehe et al. (2010) who used the principle of maximum energy dissipation (which is equivalent to MEP) to explain the observed larger density of worm burrows at the foot of the hillslope compared to the hill top. However, they were not able to explain the total number of observed worm burrows.

Another example was illustrated by Porada et al. (2011) who used MEP to constrain parameters for a physically based model based on multiple 1-D columns to simulate the water balance of the largest 35 catchments on earth. But from the six parameters that had to be tuned, they only constrained two of them by MEP (resistance for root water uptake and hydraulic conductivity), while the others were calibrated against data in a previous study (Porada et al., 2010). With this model Porada et al. (2011) ranked the different hydrological processes with respect to the produced entropy. They found that transpiration has the strongest contribution to annual average entropy production. Since their model ran on large scales, comparison between observed and simulated fluxes was only on a general basis.

Thus so far, MEP has been suggested as a promising method in hydrology, but optimized model structures have not been rigorously tested against observations: the added value of MEP for parameter estimation has not been explored yet. The aim of this paper is to tests the MEP principle along two avenues. The first is to use MEP to reduce equifinality of conceptual model structures. We used a bucket model, whose soil moisture accounting scheme is, though being simple, based on meaningful parameters. The

HESSD
9, 11551–11581, 2012

question was whether those parameter sets that maximize entropy production, under the constraint to match the water balance of HJ Andrews (the behavioural parameter sets), are realistic with respect to our knowledge about the soils in HJ Andrews? If so and if other behavioural parameter sets that do not maximize entropy production are based on parameter combinations, which are not compatible with the soils in HJ Andrews, this finding will corroborate that MEP is suitable to select the physical meaningful parameter sets within the larger set of behavioural parameter sets.

The second avenue is to optimize the model parameters to maximize entropy production without the constraint to reproduce the water balance and elaborate whether simulations with this model structure come close to the observed water balance.

This study reveals two main problems using MEP to constrain conceptual models. The first is that conceptual models are based on the idea of linear systems and different fluxes are simulated in a linear independent manner, which reduces the possibility for process interactions and trade-offs between fluxes. The second problem is that several fluxes in conceptual hydrological models are not driven by potential gradients, which is of prime importance for calculating entropy production.

2 Short introduction to MEP

In this section we give a short introduction of MEP, with an emphasis to the application of this article. For a more detailed and fundamental description of MEP, the reader is referred to e.g. Kondepudi and Prigogine (1998), Kleidon (2010b) or Kleidon et al. (2012).

The second law of thermodynamics states that entropy cannot be consumed but only produced. This is the case during irreversible processes that cannot be reversed in time. For isolated systems this implies that the system evolves to a state of maximum entropy, which implies perfect mixing. Perfect mixing means depletion of all gradients: the system is in a state of maximum disorder.

HESSD
9, 11551–11581, 2012

Open systems may, however, exchange energy and mass with their environment. Organized structures may form and persist when incoming fluxes provide the necessary free energy and entropy is exported to the environment. Persistent exchange of energy flows through the system requires a persistent driving macroscale gradient that spans across the entire system. The Bernard cell (Prigogine, 1989) but also planet Earth (Kleidon, 2010b) are prominent examples. The fluxes along such macroscale gradients would deplete their driving gradient if there would be no positive feedback. In the Bernard cell this is the heating at the bottom and cooling at the top of the cell. In the planet earth this is planetary energy exchange (the pole receive less radiation input than the equator). The MEP principle states now that such an open system in steady state is structured in such a way that it maximizes entropy production. In case of no feedback this implies that the system reaches thermodynamic equilibrium as fast as possible.

In formula form, the entropy production $\mathrm{d}S$ [$\mathrm{J\,K^{-1}}$] is given by:

$$\frac{\mathrm{d}S}{\mathrm{d}t} = \sigma - \mathrm{NEE} \tag{1}$$

where σ is the rate of entropy production that should be maximized [$\mathrm{W\,K^{-1}}$] and NEE is the net energy exchange across the borders of the system [$\mathrm{W\,K^{-1}}$]. In steady state σ = NEE and σ is given by

$$\sigma = \frac{1}{T}\frac{\mathrm{d}U + \mathrm{d}W}{\mathrm{d}t} \tag{2}$$

where U is internal energy [J], W performed work [J] and T is temperature [K]. When temperature is assumed to be constant, Eq. (2) can be written as

$$\sigma = \frac{1}{T}\frac{\mathrm{d}W}{\mathrm{d}t} = \frac{P}{T} \tag{3}$$

where P is power [$\mathrm{J\,s^{-1}}$]. This equation shows that MEP is equivalent to maximizing power.

HESSD
9, 11551–11581, 2012

Power is given as $P = \boldsymbol{F}\nabla\phi$ where $\boldsymbol{F}$ is the flux [$\mathrm{kg\,s^{-1}}$] and $\nabla\phi$ is the gradient [$\mathrm{J\,kg^{-1}}$] that drives the flux (if the flux is given in $\mathrm{m^3\,s^{-1}}$, the gradient should be given in $\mathrm{N\,m^{-2}}$). The flux is then determined by the gradient divided by the resistance of the medium. Now it can be easily shown that there exists a maximum in power, when looking at the extremes: a zero resistance and an infinite resistance. When the resistance is zero, the flux will be infinite and the gradient will be depleted immediately, resulting in zero power. On the other extreme, when the resistance is infinite, the flux will be zero which also leads to zero power. Somewhere in-between these two extremes the power will be maximum.

3 Model setup

For the MEP principle to work the system should be in steady state. We therefore focussed on the average yearly water balance, which we assume is to be steady state. We used a simple bucket model to test MEP and, at first we limited ourselves to only one bucket that represents the unsaturated soil, since the partitioning between evapotranspiration and runoff is assumed to happen here. This is in accordance with several bucket models such as e.g. the HYMOD conceptual watershed model (Moore, 1985), the HBV model (Lindström et al., 1997), the GR4J model (Perrin et al., 2003) or the SUPRFLEX model (Fenicia et al., 2011). To be able to better compare simulated with observed runoff, we added two buckets that accounts for the timing of runoff (Fig. 1).

Testing the MEP hypothesis using a bucket model along the above outlined two avenues implied two main difficulties. The first was to design a soil moisture accounting scheme that is simple but nevertheless based on interpretable parameters. The second was to define proper definitions of driving gradients, because most bucket models do not account for the gradients that driven these fluxes in a explicit manner. The used expressions for the driving gradients were thus not derived from first principles, but they were constructed on plausible reasoning. An intensive discussion on the gradients is added in Sect. 6.

HESSD
9, 11551–11581, 2012

All fluxes in the model were described in $m s^{-1}$ per unit area giving power the unit of $W m^{-2}$. The model was run on a hourly time step and solved with an implicit numerical scheme.

3.1 Unsaturated zone

The model is similar to the HBV model with the difference that we added a groundwater component in the unsaturated soil reservoir (Fig. 1). For simplicity we assumed no snowfall and interception. The water balance of the bucket is given by:

$$\frac{dS_M}{dt} = P_{eff} - E_a - Q_d - G \tag{4}$$

where S_M is the water storage in the bucket [m], P_{eff} and E_a are the effective rainfall [$m s^{-1}$] and actual evapotranspiration [$m s^{-1}$] and Q_d and G are the overland flow [$m s^{-1}$] and groundwater leakage [$m s^{-1}$], while t is time [s]. Actual evaporation and its driving gradient are given by:

$$E_a = E_{pot} \min\left(\frac{S_M}{S_{max} F_C}, 1\right) \tag{5}$$

$$\nabla_{E_a} = e_s - e_a$$

where E_{pot} is the potential evaporation [$m s^{-1}$], determined with the Penman formula (Monteith, 1981). Note that the albedo α [–] is treated as a calibration parameter. S_{max} is the maximum storage of the bucket [m], and F_C is the field capacity [–] (although this is not a soil physical field capacity, this parameter can be interpreted in a soil physical sense. Soils with high clay content store a large amount of water against gravity. Hence, F_C should be close to 0.8. Sandy soils have a low field capacity, thus F_C should be around 0.1). ∇_{E_a} is the gradient driving evaporation [$N m^{-2}$] and e_s and e_a are the saturated and actual water vapour pressure [$N m^{-2}$]. Where $e_a = H e_s$, with

HESSD
9, 11551–11581, 2012

H being relative humidity [−]. Thus, the driving gradient is defined as the water vapour demand of the atmosphere.

Overland flow and its driving gradient are given by:

$$Q_d = P_{eff}\left(\frac{S_M}{S_{max}}\right)^{\beta} \tag{6}$$

$$\nabla_{Q_d} = \frac{\rho g}{\eta} S_M \left(\frac{S_M}{S_{max}}\right)^{\beta}$$

where β is a scaling parameter accounting for the catchment heterogeneity of the depth of the unsaturated soil [−] and ∇_{Q_d} is the gradient [$N m^{-2}$] driving Q_d, while ρ, g and η are the water density [$kg m^{-3}$], gravitational acceleration [$m s^{-2}$] and soil porosity [−], respectively. The driving gradient is thus derived as the potential energy multiplied by the scaling factor $(S_M/S_{max})^{\beta}$.

Groundwater percolation and its driving gradient are given by:

$$G = K_s\left(\frac{S_M}{S_{max}}\right)^{\beta} \qquad \text{for } S_M > S_{max}F_C \tag{7}$$

$$\nabla_G = \frac{\rho g}{\eta}\max(0, S_M - S_{max}F_C)$$

where ∇_G is gradient driving G [$N m^{-2}$], and K_s is the hydraulic conductivity of the soil [$m s^{-1}$]. Please note that though being simple, this conceptualization of percolation can be parameterized in a manner that is consistent with soil physics. For instance a sandy soil has a high K_s, around values of $10^{-4}\, m s^{-1}$, in combination with a small value of F_C which leads to a physically consistent behaviour of percolation and direct runoff production. This is also the case for finer grained soils.

HESSD
9, 11551–11581, 2012

3.2 Fast runoff reservoir

The water balance for the fast runoff reservoir (middle bucket in Fig. 1) is given by:

$$\frac{dS_1}{dt} = Q_d - Q_0 - Q_1 - Q_{perc} \tag{8}$$

The fluxes and driving gradients of Q_0, Q_1 and Q_{perc} [$m s^{-1}$] are given by:

$$Q_0 = \max(S_1 - L, 0)\, k_0 \tag{9}$$

$$\nabla_{Q_0} = \frac{\rho g}{\eta} \max(S_1 - L, 0)$$

$$Q_1 = S_1 k_1 \tag{10}$$

$$\nabla_{Q_1} = \frac{\rho g}{\eta} S_1$$

$$Q_{perc} = \max(S_1, P_{max}) \tag{11}$$

where S_1 is the storage high [m], L is a storage threshold level [m] above which Q_0 becomes active, P_{max} is the maximum percolation rate to the slow reservoir [$m s^{-1}$] and k_0 and k_1 are the reservoir constants [s^{-1}]. The driving gradients are all given as a potential energy.

3.3 Slow runoff reservoir

The water balance for the fast runoff reservoir (lowest bucket in Fig. 1) is given by:

$$\frac{dS_2}{dt} = G + Q_{perc} - Q_2 \tag{12}$$

where Q_2 [$m s^{-1}$] is given by:

$$Q_2 = S_2 k_2 \tag{13}$$

$$\nabla_{Q_2} = \frac{\rho g}{\eta} S_2$$

HESSD
9, 11551–11581, 2012

where S_2 is the storage high [m] and k_2 is the reservoir constant [s^{-1}].

4 Data and calibration procedure

We applied the model to Watershed 02 of the HJ Andrews experimental forest, (latitude 44°12′43.254″ N, longitude 122°14′41.5536″ W). For a detailed description of the watershed the reader is referred to e.g. Rothacher (1965); Rothacher et al. (1967) or Tague and Band (2001). Here we give only a short description.

The watershed has a surface area of 60 ha with elevations ranging from 545 to 1070 m, and a mean slope of 30 %. The catchment is completely forested, primarily by mature Douglas fir. The underlying bedrock is volcanic material from Oligocene to lower Miocene which is overlain by a thick layer of weathered, unconsolidated material of generally high porosity (~0.6) and hydraulic conductivity (~90 m day^{-1}) (Tague and Band, 2001).

Winters are generally cool and wet, while summers are warm and dry. Precipitation over the study period ranges from 1300 to 3000 mm yr^{-1} with a mean of 2222 mm yr^{-1}. Mean runoff is 1380 mm yr^{-1}. In general, there is no seasonal snow pack in winter, but daily to weekly snow accumulation do occur.

We used meteorological data from the PRIMET station located 900 m from the site (latitude 44°12′42.8148″ N, longitude 122°15′21.3876″ W; Daly and McKee, 2011). The data set contains air temperature, solar radiation, relative humidity, precipitation and wind speed on a 1 h time step. Discharge was taken from Johnson and Rothacher (2009), also at an hourly time step. For our model we used the time series starting from 14 September 1994 until 20 August 2006, of which the first 11 months were used as a warming up period.

In a first step, we calibrated the models only to the yearly water balance. Thus, only the unsaturated zone was considered: the error in the simulation is given as $Q_{err} = \sum Q_{obs} - \sum (Q_d + G)$ [mm $year^{-1}$]. In a Monte-Carlo simulation we varied the parameters S_{max}, K_s, β, α, and F_C. This led to equifinality when reproducing the yearly

HESSD
9, 11551–11581, 2012

water balance, which we aimed to reduce by taking the MEP principle into account (which was determined by multiplying the simulated fluxes with their driving gradients).

In the second step we took two sets of parameters that reproduced the yearly water balance correctly: In one set, runoff was mainly produced by G, in the other set Q_d was the most dominant flux. With these two sets we calibrated the routing reservoirs, in which we varied the parameters k_0, k_1, k_2, L, P_{max} in a Monte Carlo approach. These results were then analysed in terms of produced power and Nash-Sutcliffe efficiency (NSE).

5 Results

5.1 Calibration on one free parameter

The hypothesis of this research was that maximizing entropy production would lead to less equifinality. In the first step we checked if an optimum in produced power in combination with a closed water balance exists when we varied only one parameter (Figs. 2 and 3). Figure 2 shows for two different sets of parameters the produced power by each flux along a range of values for S_{max}. During one realization ($\alpha = 0.2$, $K_s = 1 \times 10^{-4}$, $F_C = 0.95$ and $\beta = 5.9$, solid line), most of the total power was produced by overland flow (P_{Q_d}), while produced power by evaporation (P_E) was much smaller (for a closed water balance at $S_{max} = 630$ mm, $P_E = 15$ % of P_{tot}) and power produced by the groundwater flux (P_G) was almost $0\,W\,m^{-2}$. For another set of parameters ($\alpha = 0.45$, $K_s = 2.3 \times 10^{-5}\,m\,s^{-1}$, $F_C = 0.2$ and $\beta = 36$, dotted line) it was the other way round: P_G was large, while P_{Q_d} was almost $0\,W\,m^{-2}$. Although the second parameter set produced more power than the first set, no optimum value for S_{max} exists. Only at very large values of S_{max}, when E_a will be reduced to zero, produced power will not increase anymore.

Total power production was also highest for the case where G was dominating. Reason for this is that G is more constant over time, while Q_d only occurs at moments when

HESSD
9, 11551–11581, 2012

it rains (note that power is determined as the average value over 11 yr). At the same time, values for F_C were small, making the gradient ∇_G only little smaller than ∇_{Q_d}.

However, when we only varied β, parameter sets existed where maximum produced power coincided with a closed water balance (Fig. 3). The solid lines in Fig. 3 were obtained with the parameters $S_{max} = 500\,mm$, $\alpha = 0.46$, $K_s = 1 \times 10^{-3}\,m\,s^{-1}$ and $F_C = 0.1$. Dotted lines were simulated with parameter values of $S_{max} = 300\,mm$, $\alpha = 0.2$, $K_s = 2.3 \times 10^{-5}\,m\,s^{-1}$ and $F_C = 0.2$. Striking is that this only occurs for large values of β, implying that most runoff is produced by G. Largest total power production was obtained by the solid lines which uses $K_s = 1 \times 10^{-3}\,m\,s^{-1}$ combined with a small F_C; values that are representative for this watershed (Tague and Band, 2001). However, it could be that these results are rather a coincidence than a solid proof that maximum power production can indeed constrain such a conceptual model. This will be discussed in Sect. 6.

5.2 Calibration on two free parameters

Now we relax our constrains a bit and calibrate on two parameters at the time. Two different parameter sets were explored and the sensitivity analyses are shown as bivariate plots in Fig. 4. In the first set total power production was mainly produced by Q_d (black circle in Fig. 4), while with the second parameter set power was mainly produced by G (grey circle in Fig. 4). Bivariate plots are shown for K_s vs. F_C and S_{max} vs. β. In the first parameter set α had a value of 0.32 and in the second parameter set 0.45. Produced power is only shown for those parameter sets that have an error in the water balance of $|Q_{err}| < 15\,mm\,yr^{-1}$. Simulation with a larger $|Q_{err}|$ are plotted as light grey dots and indicate the full range of the explored parameter space. Note that α influences E_{pot} and that it was chosen in such a way that the water balance could be closed along a wide range of the parameter space.

The bivariate plots of K_s vs. F_C show the same pattern for both parameter sets, but their ranges differ. Most power was produced for high values of F_C at a point where K_s values were insensitive. This means that G was reduced to almost nothing. On the

HESSD
9, 11551–11581, 2012

other side of the spectrum (small F_C, large K_s) a local maximum in produced power is visible, which is more pronounced in the second parameter set. The second maximum in P reflects larger fluxes by G and smaller fluxes by Q_d. For intermediate values of F_C and K_s, produced power was minimum. This is also the area where Q_d and G are in the same range.

In the trade-off between S_{max} and β a clear pattern is visible with increasing power production for increasing values of S_{max}. Within parameter set 1, only for a small range of S_{max} the water balance could be closed, while β was relatively insensible. In parameter set 2, the water balance could be closed along the full range of S_{max} with maximum P at maximum S_{max}. β was rather insensitive when looking at produced power. The sensitivity of β for closing the water balance shows a different picture: for $S_{max} >\sim 500$ mm β was insensitive, while for $S_{max} <\sim 500$ mm, β was realy sensitive. Power production at these lower values of S_{max} was relatively low and insensitive.

But the most important observation with regard to the objectives of this paper was that no optimum in produced power is visible. Power was only maximum at either the lower or the upper end of a particular parameter range.

5.3 Free calibration

Now, we move to free calibration of all five parameters that control the unsaturated zone. If our hypothesis that the MEP principle could constrain the behavioural parameter set is correct, a clear optimum in power should coincide with a closed water balance. However, this was not the case (Fig. 5): power was large for large values of S_{max} and α, and for small values of K_s. For F_C and β the largest values of P were more spread over the parameter space and did not show a clear optimum in power production. Large values of power did also not coincide consistently with a closed water balance (note that Fig. 5 only shows a relatively small range of Q_{err}). Also in the case of free calibration, for parameter sets that produced large power, power was mainly produced by either Q_d or G. Parameter sets that produced more or less equal shares of Q_d and G produced less power. For all different parameter sets, E_a produced only 1 to 15 % of the total

HESSD
9, 11551–11581, 2012

power. The reason for the small portion of power produced by E_a is that the defined gradient ∇_{E_a} was an order of magnitude lower than either ∇_{Q_d} or ∇_G.

5.4 Calibration of routing reservoirs

In the last step we took two parameter sets of the unsaturated zone that reproduced the water balance correctly and tried to constrain the parameters defining the lower two reservoirs. One parameter set mainly produced runoff by Q_d (black circles in Fig. 4) and in the other parameter set G was the main responsible for runoff generation (grey circles in Fig. 4).

In a Monte-Carlo run we varied the parameters that described the two lower reservoirs. For both parameter sets, a large NSE corresponds with little produced power and vice versa, with more scatter in the first parameter set (Figs. 6a and 7a). The latter is due to the fact that, in the G-dominating parameter set, most water was directed straight to the slow runoff reservoir, making the parameters L, k_{perc}, k_1 and k_2 insensitive, while in the first parameter set all five parameters had an influence.

The trade-off between P and NSE is best seen in the G-dominated case (Fig. 7a). Reason for this is that in the (in this case) lower reservoir, there was no trade-off between different fluxes. If k_2 gets smaller, S_2 should increase to match the yearly water balance. A larger gradient in combination with an (on average) same flux results in larger power production. This can also be seen by comparing Fig. 6b with 6c or Fig. 7b with 7c. The hydrographs that produced most power (Figs. 6c and 7c) are almost constant over time. Note that if the values of k_0, k_1 and k_2 go towards zero, S_1 and S_2 would go to infinity, Q_{tot} would become completely constant and P would be maximum. Thus also for the routing reservoirs, the MEP principle cannot constrain the parameter set in a meaningful way.

HESSD
9, 11551–11581, 2012

6 Discussion

Our results show that we were not able to constrain our model by using the MEP principle. A reason for this failure can be that the hypothesis that nature strives to a state of MEP is not correct. But if we assume that the principle is correct, our test should be incomplete. And we do believe that our test is incomplete. We first need to have faith in our test to be able to accept or reject the MEP hypothesis. To do so, the model should at least (1) be thermodynamically consistent: i.e. fluxes should be described as gradients divided by resistances, (2) have trade-offs between different processes and (3) have the right degrees of freedom.

6.1 Flux = gradient/resistance

To be consistent with thermodynamic principles, each flux in the model should be defined as a gradient divided by a resistance (or multiplied by a conductivity), and the flux should have a feedback to its gradient: i.e. a larger flux depletes the gradient faster, and, consequently, the flux will be smaller. The resistance is than treated as the unknown that can be solved with the MEP principle. Note that a gradient should in principle be unitless (i.e. $\mathrm{m\,m^{-1}}$). However, it can be defined as a height difference or an energy difference when the resistance is given in s (or conductivity in $\mathrm{s^{-1}}$, as is the case for reservoir constants).

Our model concept is often not consistent with thermodynamics. An obvious one is Q_d. Of course, S_M is part of the driving gradient, but as long as it not raining, Q_d and S_M have no connection at all, let alone a feedback. And even more obvious is that a resistance term is lacking in the formulation of Q_d.

Another possible description for the gradient of free water flow is the potential energy difference between a point in the catchment and the outlet of the catchment as is done by e.g. Porada et al. (2011). Although the gradient seems better described, the feedback is often limited: in steep areas the gradient will remain almost constant, since

HESSD
9, 11551–11581, 2012

it is mainly the topography (and only to a small extend the water level) that determines the gradient.

Another flux that is not described in a thermodynamic consistent manner is actual evaporation. We described the gradient as atmospheric water demand. Even though this term is part of the used Penman formula to determine potential evaporation, the feedback with the flux is missing. This is because this term is determined by observations (i.e. temperature and relative humidity) that have been measured at 1.50 m above ground surface. In principle, there will be a feedback between atmospheric water demand and transpiration, since relative humidity increases with increasing transpiration. However, this is only noticeable in the thin boundary layer around the leaves. Only if we can simulate the relative humidity of this thin boundary layer, one may have a feedback between transpiration and atmospheric water demand.

Nevertheless, we implemented a feedback between E_a and S_M, but this was not reflected in ∇_{E_a}. This may be included by defining driving gradients as differences between chemical potentials as was done by e.g. Porada et al. (2011). But in a similar way as we did, they also used a linear feedback between the actual and maximum water storage. Such a feedback is definitely the easiest, but therefore not necessarily the correct feedback. And there is still no feedback between transpiration and atmospheric water demand.

As a last example of our thermodynamic inconsistency we mention the coupling of the different reservoirs. In our current setup, no feedbacks are present between the different reservoirs. In the routing reservoirs, the water level can increase to infinity without affecting "upstream" reservoirs. Only when a flux depends on the state in its reservoir of origin ánd on that of its destination, one may have a proper feedback.

6.2 Trade-offs between processes

A second necessity when applying the MEP principle is that there should be a trade-off between two or more different fluxes or processes. This was especially lacking in the slow runoff reservoir, resulting in MEP when the conductivity goes to zero.

HESSD
9, 11551–11581, 2012

But also when there are trade-offs between fluxes, the MEP principle can only be applied when the resistance of all but one flux is given. Only one resistance will then be optimized with MEP (Kleidon and Schymanski, 2008). To be able to optimize two resistances of two competing fluxes, Porada et al. (2011) used an iterative approach where in the first step one resistance is optimized for given values of the other resistance, and vice versa. Subsequently they state that the optimum value of both resistances are on the two "ridges" of the two optima (Fig. 4 of Porada et al., 2011). This is an interesting approach, but a "proof" or explanation why the optimum should be on the ridges is missing in their approach.

6.3 What are the right degrees of freedom?

The last issue discussed here touches the point on where to define the model boundaries and which processes should be described in detail. First of all one should keep in mind that the MEP principle only applies for steady state conditions. But in hydrology (and in almost any natural system) a system that is really in steady state does not exist. Thus one should choose a timescale over which it can be assumed that the system is close to steady state. In our model concept we chose a year, but it has to be seen if this is the most appropriate time scale (if there exist one). It may be that in some cases a single rainstorm is a better time scale (e.g. Zehe et al., 2010).

Another choice should be made on which processes to add to your model. As hydrologists we are mainly concerned about water fluxes. However, many other processes influence these fluxes by influencing either the gradients or the resistances. Including these processes and describing them correctly is difficult and may requires knowledge from totally different fields of expertise.

An example in our model concept is that of transpiration. We used the Penman formula in which the energy availability is reflected in the a priori calculation of the potential evaporation. Implicitly, we assume that transpiration is water limited, which does not seem to be the case in the HJ Andrews. In humid areas, transpiration is rather energy limited and in some cases nutrient limited (e.g. the Amazon). The key is thus to find

HESSD
9, 11551–11581, 2012

the real limiting factors and their negative feedbacks. Schymanski et al. (2009b) used the fact that, to increase transpiration, a plant needs more leaves for photosynthesis. Building these cost energy and at one point leaves can only be in the shadow of other leaves, which reduces the leave's efficiency. They used this trade off as an optimality principle to estimate transpiration. Their study was only tested in a subhumid region in Northern Territory, Australia, thus further research is required to apply this concept in humid regions.

Besides optimality of a single plant, also competition between plants or between plant species may be important to add as a process.

Another example that can have a large influence on the local hydrology is the creation of macropores. However, it is difficult to describe all processes that creates and limits the amount of macropores. For example, Zehe et al. (2010) show that worm burrows in the soil allow for faster fluxes against very steep gradients and that a higher density of worm burrows at the foot of the hillslope is, in a thermodynamic sense, more favourable than at the top of the hillslope (which is in agreement with their observations). However, the higher the density of worm burrows, the higher is the production of entropy during rainfall events. The optimum is thus an infinite number of worm burrows, which is of course not possible. Reason for this model behaviour is that no negative feedback on the persistence of the worm burrows or on the total worm population was implemented.

Thus to test the MEP principle, a model is needed that accounts for the real degrees of freedom which may be different for each process, catchment, or timescale.

7 Conclusions

In this study we tried to use MEP to constrain a simple hydrological bucket model. We showed that we could optimize β with MEP, and that this optimized parameter set is consistent with what we know of the tested catchment, which seemed promising. However, this was the only parameter for which we found an optimum, and for reasons discussed in Sect. 6, we believe that this is rather a coincidence than an inevitable

HESSD
9, 11551–11581, 2012

result of our approach. We conclude that constraining the current model with MEP did not work. Besides the fact that the MEP hypothesis may be wrong, we mentioned several shortcomings in our approach to apply the MEP principle in a (potentially) correct manner.

Many of these shortcomings origin from the fact that we seem not to have understood the MEP principle correctly, while a model that do fulfil the important requirements mentioned in the discussion, would (hopefully) lead to a better result. The reason for us to still describe the current, thermodynamically inconsistent model, is that it reflects our own learning curve, and we believe that learning from mistakes and failures is an effective way to learn. At the same time, only little literature exists about hydrological applications of MEP and when exploring these principles one may easily make similar mistakes as we did. Thus we hope that this article helps to understand the MEP principles in a better way and that it prevent others from making the same mistakes as we did.

Although we were not able to test the MEP principle in a proper way, we discussed several points on how to improve the test. In summary, this is (without the guarantee that this list is sufficient!):

1. The system should be in a steady state (or at least close to it).
2. Fluxes should be described by a gradient divided by a resistance.
3. There should be feedbacks between fluxes and gradients.
4. There should always be a trade-off between two or more fluxes.
5. The MEP principle can only optimize the resistance of one flux.
6. Each process should have the right degrees of freedom.

The last point is probably the most difficult one and depends on the process described and the timescale applied. Often, knowledge from other disciplines such as ecology or biology may be needed. The steady state assumption is also a critical assumption

HESSD
9, 11551–11581, 2012

which is, by definition, violated. The change in the system may only be small enough to have no influence on the final result. An interesting question for further research is if the MEP principle also holds in steady state systems that have a periodic input signal. This is a critical point since the atmospheric input is, at best, periodic.

Furthermore, we would like to stress that with this study we do not claim that the MEP principle does not work, but we showed that applying the principle is not as straight forward as it may seem. Only if is applied it in a correct way, while having the correct constraints, one will be able to test the MEP principle. If that point is reached, and if the MEP principle still holds, it would mean a big step forward in the hydrological science.

Acknowledgements. Data sets were provided by the HJ Andrews Experimental Forest research program, funded by the National Science Foundation's Long-Term Ecological Research Program (DEB 08-23380), US Forest Service Pacific Northwest Research Station, and Oregon State University.

The service charges for this open access publication have been covered by a Research Centre of the Helmholtz Association.

References

Brolsma, R. J. and Bierkens, M. F. P.: Groundwater-soil water-vegetation dynamics in a temperate forest ecosystem along a slope, Water Resour. Res., 43, W01414, doi:10.1029/2005WR004696, 2007. 11553

Caylor, K. K., Scanlon, T. M., and Rodriguez-Iturbe, I.: Ecohydrological optimization of pattern and processes in water-limited ecosystems: a trade-off-based hypothesis, Water Resour. Res., 45, W08407, doi:10.1029/2008WR007230, 2009. 11553

Clark, M. P., Kavetski, D., and Fenicia, F.: Pursuing the method of multiple working hypotheses for hydrological modeling, Water Resour. Res., 47, W09301, doi:10.1029/2010WR009827, 2011. 11553

HESSD

9, 11551–11581, 2012

Daly, C. and McKee, W.: Meteorological data from benchmark stations at the Andrews Experimental Forest, Long-Term Ecological Research, Forest Science Data Bank, Corvallis, OR, [Database], available at: http://andrewsforest.oregonstate.edu/data/abstract.cfm?dbcode=MS001, last access: 22 November 2011. 11561

Dewar, R. C.: Maximum entropy production as an inference algorithm that translates physical assumptions into macroscopic predictions: don't shoot the messenger, Entropy, 11, 931–944, doi:10.3390/e11040931, 2009. 11553

Dewar, R. C.: Maximum entropy production and plant optimization theories, Philos. T. Roy. Soc. B, 365, 1429–1435, doi:10.1098/rstb.2009.0293, 2010. 11553, 11554

Fenicia, F., Kavetski, D., and Savenije, H. H. G.: Elements of a flexible approach for conceptual hydrological modeling: 1. Motivation and theoretical development, Water Resour. Res., 47, W11510, doi:10.1029/2010WR010174, 2011. 11557

Johnson, S. and Rothacher, J.: Stream discharge in gaged watersheds at the Andrews Experimental Forest. Long-Term Ecological Research, Forest Science Data Bank, Corvallis, OR [Database], available at: http://andrewsforest.oregonstate.edu/data/abstract.cfm?dbcode=HF004 (last access: 22 November 2011), 2009. 11561

Klausmeier, C. A.: Regular and irregular patterns in semiarid vegetation, Science, 284, 1826–1828, doi:10.1126/science.284.5421.1826, 1999. 11554

Kleidon, A.: Nonequilibrium thermodynamics and maximum entropy production in the Earth system, Naturwissenschaften, 96, 653–677, doi:10.1007/s00114-009-0509-x, 2009. 11553

Kleidon, A.: A basic introduction to the thermodynamics of the Earth system far from equilibrium and maximum entropy production, Philos. T. Roy. Soc. B, 365, 1303–1315, doi:10.1098/rstb.2009.0310, 2010a. 11553

Kleidon, A.: Life, hierarchy, and the thermodynamic machinery of planet Earth, Phys. Life Rev., 7, 424–460, doi:10.1016/j.plrev.2010.10.002, 2010b. 11553, 11555, 11556

Kleidon, A. and Schymanski, S.: Thermodynamics and optimality of the water budget on land: a review, Geophys. Res. Lett., 35, L20404, doi:10.1029/2008GL035393, 2008. 11553, 11554, 11568

Kleidon, A., Zehe, E., Ehret, U., and Scherer, U.: Thermodynamics, maximum power, and the dynamics of preferential river flow structures on continents, Hydrol. Earth Syst. Sci. Discuss., 9, 7317–7378, doi:10.5194/hessd-9-7317-2012, 2012. 11555

Kondepudi, D. and Prigogine, I.: Modern Thermodynamics: From Heat Engines to Dissipative Structures, Wiley, Chichester, 1998. 11555

HESSD
9, 11551–11581, 2012

Lindström, G., Johansson, B., Persson, M., Gardelin, M., and Bergström, S.: Development and test of the distributed HBV-96 hydrological model, J. Hydrol., 201, 272–288, doi:10.1016/S0022-1694(97)00041-3, 1997. 11557

Lorenz, R. D., Lunine, J. I., Withers, P. G., and McKay, C. P.: Titan, Mars and Earth: entropy production by latitudinal heat transport, Geophys. Res. Lett., 28, 415–418, doi:10.1029/2000gl012336, 2001. 11553

McDonnell, J., Sivapalan, M., Vaché, K., Dunn, S., Grant, G., Haggerty, R., Hinz, C., Hooper, R., Kirchner, J., Roderick, M., Selker, J., and Weiler, M.: Moving beyond heterogeneity and process complexity: a new vision for watershed hydrology, Water Resour. Res., 43, W07301, doi:10.1029/2006WR005467, 2007. 11552, 11553

Monteith, J. L.: Evaporation and surface temperature, Q. J. Roy. Meteorol. Soc., 107, 1–27, doi:10.1002/qj.49710745102, 1981. 11558

Moore, R. J.: The probability-distributed principle and runoff production at point and basin scales, Hydrolog. Sci. J., 30, 273–297, doi:10.1080/02626668509490989, 1985. 11557

Paik, K. and Kumar, P.: Optimality approaches to describe characteristic fluvial patterns on landscapes, Philos. T. Roy. Soc. B, 365, 1387–1395, doi:10.1098/rstb.2009.0303, 2010. 11553

Paltridge, G. W.: Climate and thermodynamic systems of maximum dissipation, Nature, 279, 630–631, doi:10.1038/279630a0, 1979. 11553

Perrin, C., Michel, C., and Andréassian, V.: Improvement of a parsimonious model for streamflow simulation, J. Hydrol., 279, 275–289, doi:10.1016/S0022-1694(03)00225-7, 2003. 11557

Porada, P., Arens, S., Buendía, C., Gans, F., Schymanski, S. J., and Kleidon, A.: A Simple Global Land Surface Model for Biogeochemical Studies, Tech. Rep. 18, Max-Planck-Institut für Biogeochemie, Jena, Germany, 2010. 11554

Porada, P., Kleidon, A., and Schymanski, S. J.: Entropy production of soil hydrological processes and its maximisation, Earth Syst. Dynam., 2, 179–190, doi:10.5194/esd-2-179-2011, 2011. 11554, 11566, 11567, 11568

Porporato, A., Laio, F., Ridolfi, L., and Rodriguez-Iturbe, I.: Plants in water-controlled ecosystems: active role in hydrologic processes and response to water stress: III. Vegetation water stress, Adv. Water Resour., 24, 725–744, doi:10.1016/S0309-1708(01)00006-9, 2001. 11553

Prigogine, I.: What is entropy?, Naturwissenschaften, 76, 1–8, doi:10.1007/BF00368303, 1989. 11556

HESSD
9, 11551–11581, 2012

Rodriguez-Iturbe, I., D'Odorico, P., Porporato, A., and Ridolfi, L.: On the spatial and temporal links between vegetation, climate, and soil moisture, Water Resour. Res., 35, 3709–3722, doi:10.1029/1999WR900255, 1999. 11553

Rothacher, J.: Streamflow from small watersheds on the western slope of the Cascade Range of Oregon, Water Resour. Res., 1, 125–134, doi:10.1029/WR001i001p00125, 1965. 11561

Rothacher, J., Dyrness, C. T., and Fredriksen, R. L.: Hydrologic and related characteristics of three small watersheds in the Oregon Cascades, US Department of Agriculture, US Forest Service, Pacific Northwest Research Station, Portland, Oregon, USA, 1967. 11561

Schaefli, B., Harman, C. J., Sivapalan, M., and Schymanski, S. J.: HESS Opinions: Hydrologic predictions in a changing environment: behavioral modeling, Hydrol. Earth Syst. Sci., 15, 635–646, doi:10.5194/hess-15-635-2011, 2011. 11553

Schymanski, S. J., Kleidon, A., and Roderick, M. L.: Ecohydrological optimality, in: Encyclopedia of Hydrological Sciences, edited by: Anderson, M. G., vol. 1, John Wiley & Sons Ltd., doi:10.1002/0470848944.hsa319, 2009a. 11553

Schymanski, S. J., Sivapalan, M., Roderick, M. L., Hutley, L. B., and Beringer, J.: An optimality-based model of the dynamic feedbacks between natural vegetation and the water balance, Water Resour. Res., 45, W01412, doi:10.1029/2008WR006841, 2009b. 11553, 11569

Schymanski, S. J., Kleidon, A., Stieglitz, M., and Narula, J.: Maximum entropy production allows a simple representation of heterogeneity in semiarid ecosystems, Philos. T. Roy. Soc. B, 365, 1449–1455, doi:10.1098/rstb.2009.0309, 2010. 11554

Tague, C. L. and Band, L. E.: Evaluating explicit and implicit routing for watershed hydro-ecological models of forest hydrology at the small catchment scale, Hydrol. Process., 15, 1415–1439, doi:10.1002/hyp.171, 2001. 11561, 11563

Thompson, S., Harman, C., Troch, P., Brooks, P., and Sivapalan, M.: Spatial scale dependence of ecohydrologically mediated water balance partitioning: a synthesis framework for catchment ecohydrology, Water Resour. Res., 47, W00J03, doi:10.1029/2010WR009998, 2011. 11553

Zehe, E. and Sivapalan, M.: Threshold behaviour in hydrological systems as (human) geo-ecosystems: manifestations, controls, implications, Hydrol. Earth Syst. Sci., 13, 1273–1297, doi:10.5194/hess-13-1273-2009, 2009. 11553

Zehe, E., Blume, T., and Blöschl, G.: The principle of maximum energy dissipation: a novel thermodynamic perspective on rapid water flow in connected soil structures, Philos. T. Roy. Soc. B, 365, 1377–1386, doi:10.1098/rstb.2009.0308, 2010. 11554, 11568, 11569

HESSD
9, 11551–11581, 2012

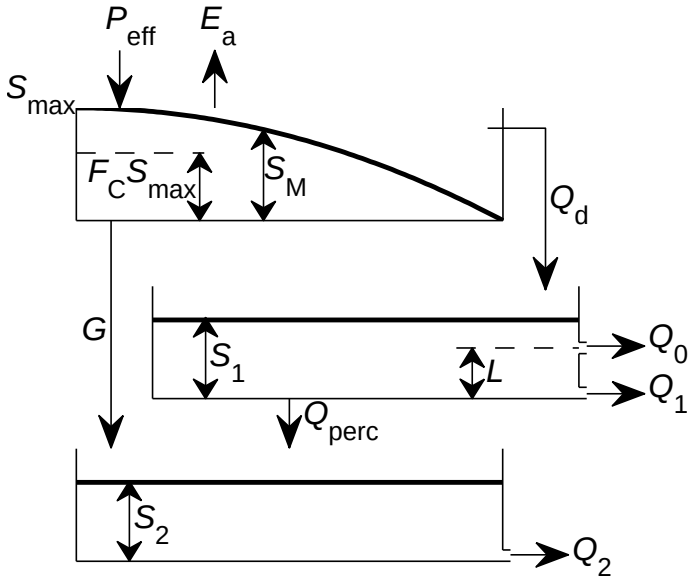

Fig. 1. Model setup. For meaning of the variables, see Sect. 3.

HESSD
9, 11551–11581, 2012

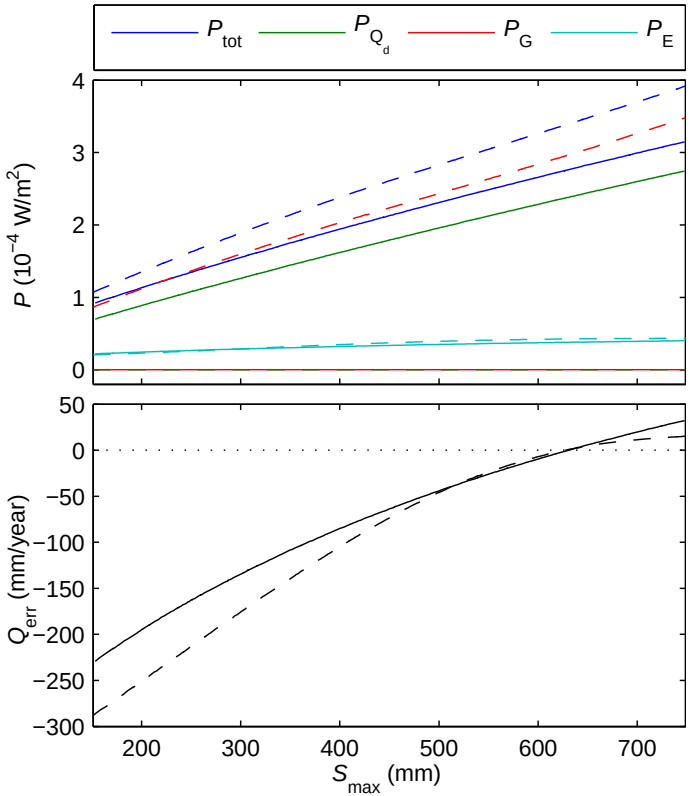

Fig. 2. Total power (P) and power produced by the different fluxes, and the error in the observed water balance (Q_{err}) along a range of S_{max}. Solid lines were simulated with parameter values of $\alpha = 0.2$, $K_s = 1 \times 10^{-4}$ m s^{-1}, $F_C = 0.95$ and $\beta = 5.9$. Dotted lines were simulated with parameter values of $\alpha = 0.45$, $K_s = 2.3 \times 10^{-5}$ m s^{-1}, $F_C = 0.2$ and $\beta = 36$.

HESSD
9, 11551–11581, 2012

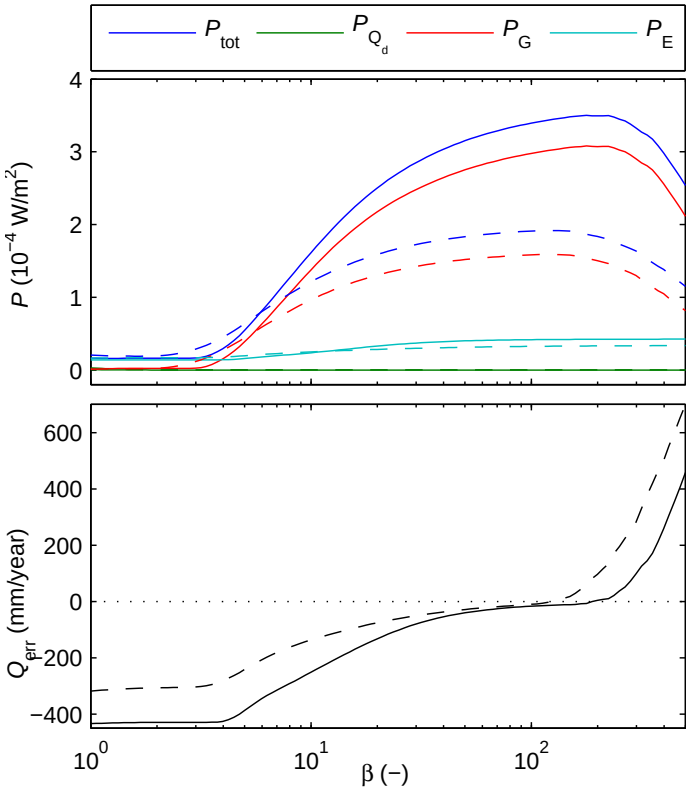

Fig. 3. Total power (P) and power produced by the different fluxes, and the error in the observed water balance (Q_{err}) along a range of β. Solid lines were simulated with parameter values of S_{max} = 500 mm, α = 0.46, $K_s = 1 \times 10^{-3}$ m s^{-1} and F_C = 0.1. Dotted lines were simulated with parameter values of S_{max} = 300 mm, α = 0.2, $K_s = 2.3 \times 10^{-5}$ m s^{-1} and F_C = 0.2.

HESSD
9, 11551–11581, 2012

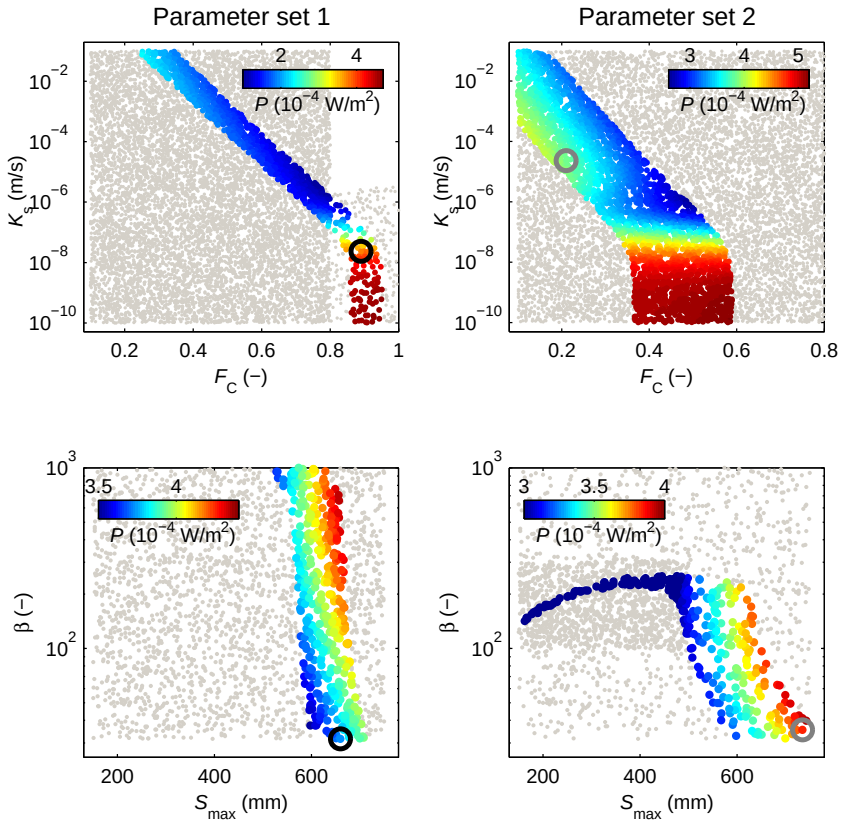

Fig. 4. Bivariate plots for two different parameter sets defining the unsaturated zone. Each grey dot represents a model run, while only the runs that have error in the simulated discharge that is smaller than 15 mm yr^{-1}, are plotted as coloured dots indicating the produced power (P). For both parameter sets, the black (and grey) circles indicate the initial parameter values. The albedo is 0.32 and 0.45 for parameter set 1 and 2, respectively. Note that the colour scale for P is different for each plot.

HESSD
9, 11551–11581, 2012

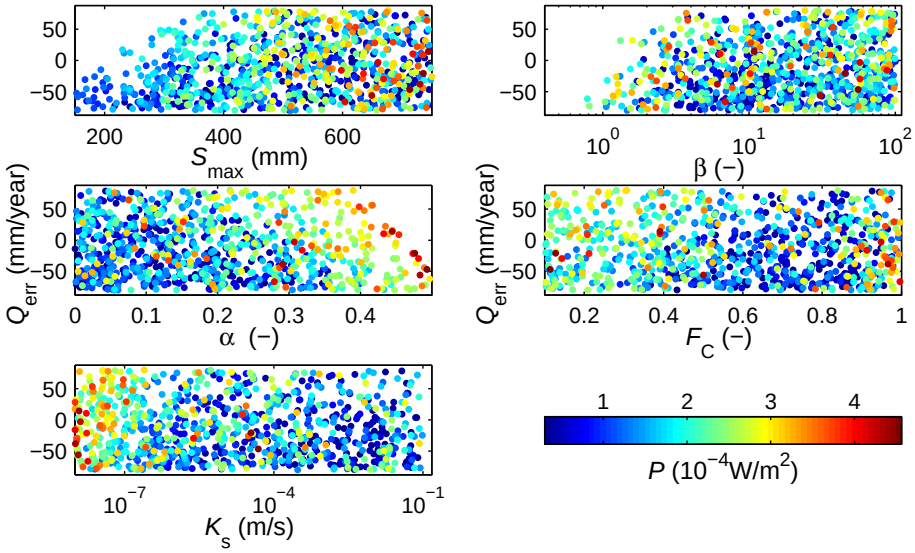

Fig. 5. Sensitivity of model parameters describing the unsaturated zone. Each dot is a model run. Power (P) is indicated in a colour scale. Q_{err} is defined as observed minus simulated discharge.

HESSD
9, 11551–11581, 2012

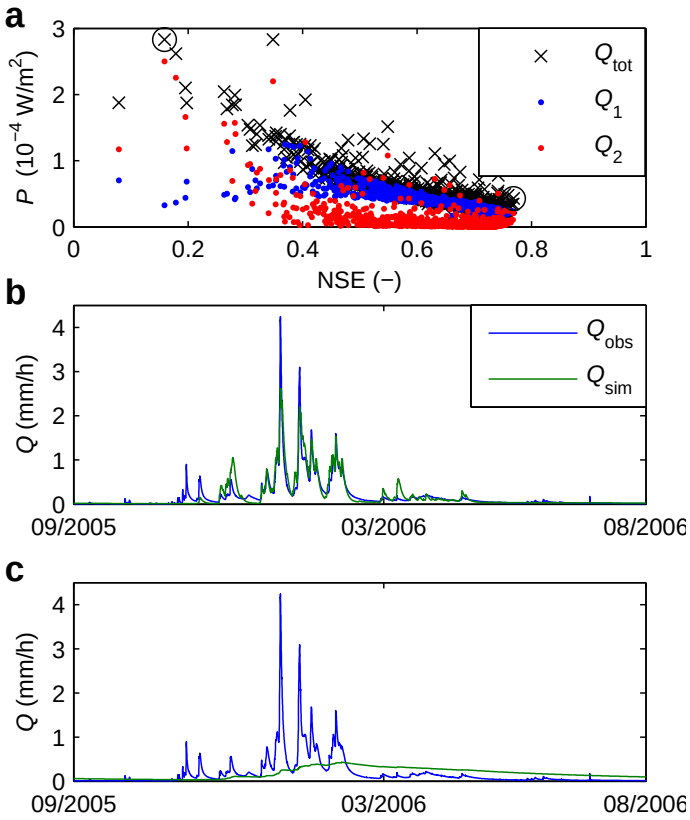

Fig. 6. Produced power by the routing reservoirs when the water balance is dominated by Q_d, with **(a)** produced power (P) vs. the Nash-Sutcliffe Efficiency (NSE), **(b)** simulated discharge at maximum NSE, and **(c)** simulated discharge at maximum power. Black circles in **(a)** denote the simulations showed in **(b)** and **(c)**.

HESSD
9, 11551–11581, 2012

MEP to constrain hydrological models

M. C. Westhoff and E. Zehe

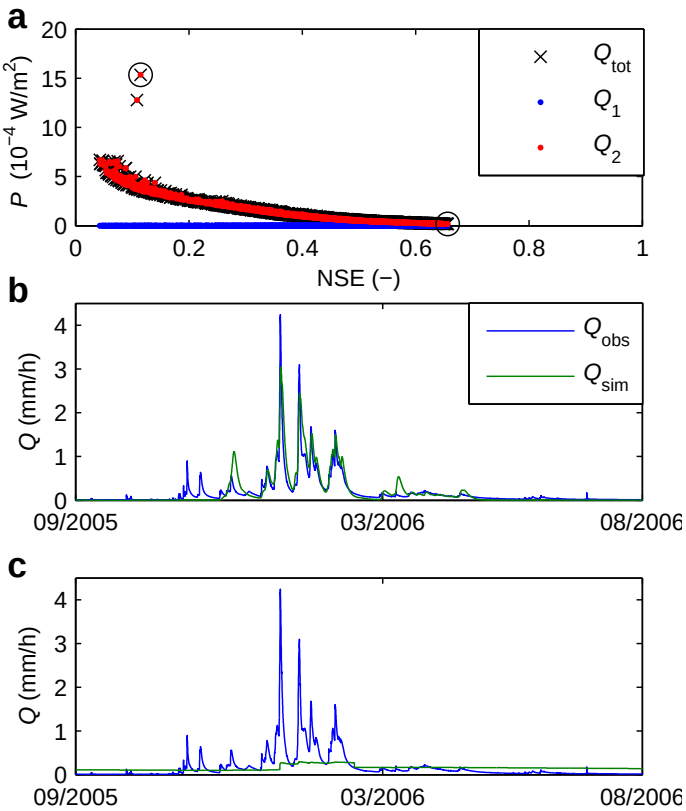

Fig. 7. Produced power by the routing reservoirs when the water balance is dominated by G, with **(a)** produced power (P) vs. Nash-Sutcliffe Efficiency (NSE), **(b)** simulated discharge at maximum NSE, and **(c)** simulated discharge at maximum power. Black circles in **(a)** denote the simulations showed in **(b)** and **(c)**.

HESSD
9, 11551–11581, 2012